

*Final version for publication*

## **Frost Damage of Roof Tiles in Relatively Warm Areas in Japan: Influence of Surface Finish on Water Penetration**

Chiemi Iba<sup>1</sup>, Shuichi Hokoi<sup>2</sup>

### **ABSTRACT**

In Japan, frost damage has been observed in relatively warm areas such as Kyoto. Spalling and fine flaking of roof tile surfaces are a typical examples of frost damage in warm areas.

In this study, the characteristics and causes of frost damage in roof tiles were investigated through water penetration experiments, freezing–thawing tests, and a numerical analysis by focusing on the moisture accumulation and freezing.

First, the methods and results of water penetration experiments were reviewed. The distribution of water in tiles was experimentally examined, and the results showed that the water content might increase in particular small areas. As the results, non-uniform moisture distributions are observed in the specimens.

Second, a new freezing–thawing test method using different water supplies was reviewed. The results of new test showed that even small water droplets could penetrate the finish and could cause spalling similar to that found in the field. These experimental results suggested that small spallings or fine flakings may occur due to the increase in water content in particular small areas due to water penetration through invisible pinholes.

The influence of pinhole on the water penetration was investigated by numerical analysis. In the analysis, the time profile and distributions of liquid water and ice contents in the freezing–thawing process were analyzed. The influence of the position of the surface finish and water permeability of the tile body was also considered. The results showed that when the water permeability was low, high local water content tended to occur, and this high water content increased the risk of frost damage.

### **1. INTRODUCTION**

Moisture in building materials significantly influences the durability of building envelopes. In cold regions, accumulated moisture occasionally freezes in the building materials, severely damaging them. In Japan, frost damage has been observed not only in cold regions but also in relatively warm areas such as Kyoto. Usually, roofs are exposed to the sky; thus, its temperature is significantly influenced by night-sky radiations (Iba and Hokoi 2003 and 2006).

Field surveys clarified that minor spalling of the roof tile surface is a typical example of frost damage in warm areas, and similar damages were observed using a new freezing–thawing test (Iba and Hokoi 2011). Two types of water penetration experiments revealed that such minor spallings occur owing to an increase in water content in particular small areas. In this paper, first, the methods and results of the

---

<sup>1</sup> Chiemi Iba, Researcher, Hokkaido Research Organization, Asahikawa, Japan

<sup>2</sup> Shuichi Hokoi, Professor, Kyoto University, Kyoto, Japan

water penetration experiments and a freezing–thawing test are reviewed.

Japanese roof tiles generally have a surface finish, in which the moisture transport property is significantly different from that of the main body, to prevent rain water penetration (Iba and Hokoi 2009). In the latter half of this paper, a numerical analysis of the freezing–thawing process focusing on the surface finish and moisture permeability is described. Furthermore, the relationship between moisture distribution and ice formation is investigated.

## 2. REVIEW OF PREVIOUS EXPERIMENTS

### 2.1 Water Penetration Experiments

To examine the water absorption characteristics of tiles, two simple experiments were performed; one in an outdoor environment and the other in a laboratory. In the outdoor experiment, four roof tiles were arranged so as to simulate an inclined roof and were exposed to outdoor conditions as shown in Figure 1. The weather was cloudy with intermittent rain. Figure 2 shows a section of the tile cut after exposure. The area that absorbed water is clearly distinguished, and the water content distribution is not uniform even in a single tile under actual climatic conditions.

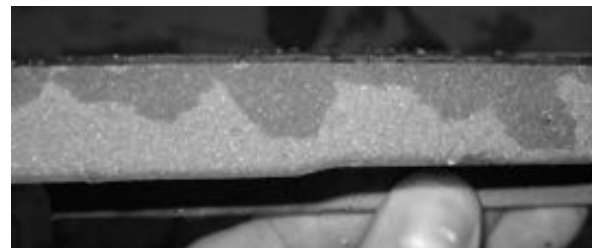


FIGURE 1: Test specimens placed outdoors      FIGURE 2: Sections of the specimen

In the laboratory experiment, water was supplied to the specimen by placing a fully wet towel on the surface so that the water could be supplied without excessive pressure as shown in Figure 3. A section of the specimen obtained 9 h after the start of the experiment is shown in Figure 4. Non-uniform water distribution was also observed.

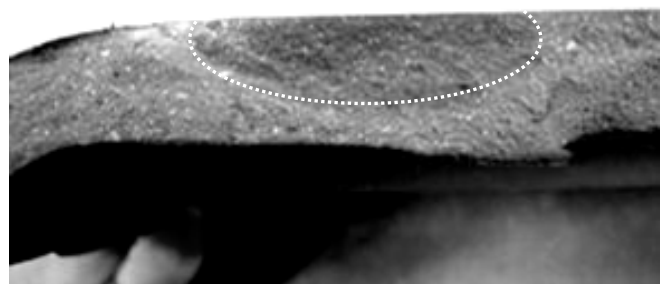


FIGURE 3: Wet towel placed on the surface      FIGURE 4: Sections of the specimen after 9 h

A previous measurement of the water resistance of a surface finish clarified that although the resistance of the finish was much higher than that of the tile body, a small amount of water could penetrate through the finish.

From the results of these two experiments, it was concluded that the water distribution does not necessarily correspond to small visible cracks or scratches on the surface finish. Therefore, it seems plausible that water penetrates through invisible pinholes on the surface.

The results of the experiments showed that the water content might increase in particular small areas. This suggests that this type of non-uniform moisture distribution leads to damages such as small spalling.

## 2.2 The New Freezing–Thawing Test

The standard freezing–thawing test method, in which the test specimen is fully saturated with water before the freezing–thawing cycles, is not suitable for evaluating the actual damage to roof tiles. Because when the standard method is used, larger and more serious cracks occur in test specimens than those found in the field survey (Iba and Hokoï 2011).

To investigate the influence of water absorption on tile deterioration under actual climatic conditions, a new freezing–thawing test was designed and conducted. The four types of water supplies shown in Figure 5 were used in this experiment. Each type is named as Pattern 1, 2, 3 and 4, respectively.

In Pattern 1, only surface condensation occurs. The water drops condensed on the upper surface of the specimen in Patterns 2 and 4. In Patterns 3 and 4, the lower surface of the specimen is immersed approximately 5 mm below the water surface. The amount of water supplied successively increases from Patterns 1 to 4.

A test apparatus based on RILEM TC 176, “Test Methods of Frost Resistance of Concrete,” was used. The temperature of an antifreeze solution was controlled at  $-20^{\circ}\text{C}$  during the freezing process and at  $+20^{\circ}\text{C}$  during the thawing process. One cycle is 12 h.

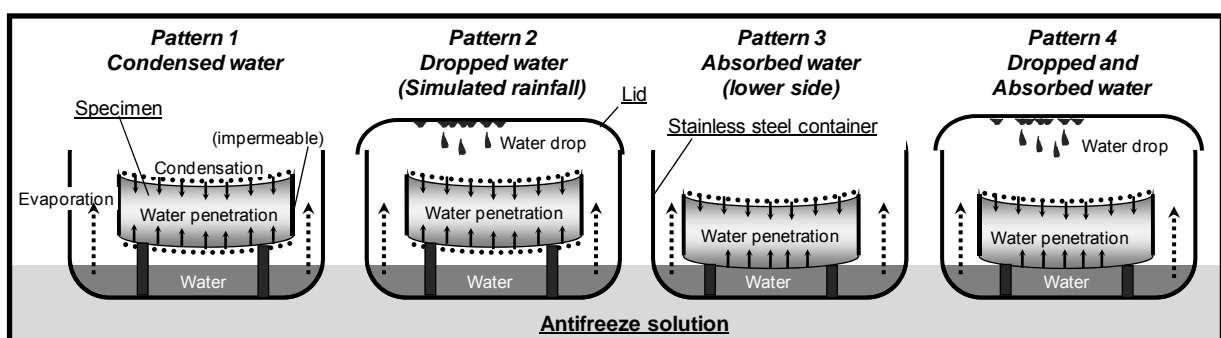


FIGURE 5: Four types of water supplies

Figure 6 shows the appearance of the specimens in Patterns 3 and 4 after 56 cycles. Fine flaking appeared and increased to cover the entire lower surface as the cycles continued. Furthermore, spallings occurred near the ends of the upper surface, although the upper surface was not immersed in water throughout the experiment.

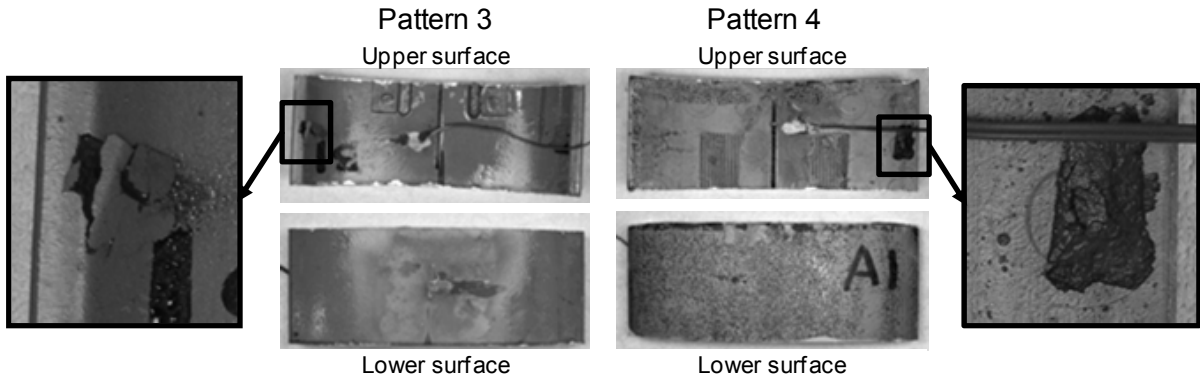


FIGURE 6: Appearance of specimens in Patterns 3 and 4 after 56 cycles

In Patterns 1 and 2, no apparent damage was found in the specimens after 56 cycles. After 90 cycles, damage similar to that in Pattern 4 was found in Pattern 2, where many fine flakes (approximately 1mm in size) appeared on the lower surface.

Since fine flakes or some damage did not appear on the lower surface in Pattern 3, the influence of water touching the bottom part of the specimen could not be clarified.

These results show that if droplets continuously fall on the specimens, even small droplets can penetrate the main body through the surface finish and can cause spalling similar to that found under actual conditions.

### 3. NUMERICAL ANALYSIS OF THE FREEZING–THAWING PROCESS

The results of the experiments described in Section 2 suggest that small spillings or fine flakings may occur due to the increase in water content in particular small areas. Furthermore, invisible pinholes could cause such high-water content.

A numerical analysis was performed to investigate the moisture transfer in the tile and to estimate the distribution of ice formation during the freezing process. This analysis does not present the preceding experimental condition but emphasize the non-uniform moisture distribution due to water penetration through a pinhole.

The influences of the surface finish and moisture permeability were also examined.

#### 3.1 Basic Equations

The equations for simultaneous heat and moisture transfer, which consider freezing and thawing, are used for the analysis (Matsumoto et al. 1993). The basic equations are as follows:

Moisture balance

$$\frac{\partial \rho_i \psi_i}{\partial t} = \nabla \cdot (\lambda'_{Tg} \nabla T) + \nabla \cdot \{ (\lambda'_{\mu g} + \lambda'_{\mu l}) \nabla \mu \} - \frac{\partial \rho_i \psi_i}{\partial t} \quad (1)$$

Energy balance

$$c \rho \psi \frac{\partial T}{\partial t} = \nabla \cdot (\lambda \nabla T) + H_{gl} \{ \nabla \cdot (\lambda'_{Tg} \nabla T) + \nabla \cdot (\lambda'_{\mu g} \nabla \mu) \} + H_{li} \frac{\partial \rho_i \psi_i}{\partial t} \quad (2)$$

Freezing condition

$$\mu = H_{li} \log_e \left( \frac{T}{T_o} \right) \quad (3)$$

where

T = absolute temperature, K

T<sub>0</sub> = freezing temperature of free water (=273.16), K

c = specific heat, J/(kg × K)

t = time, s

λ = thermal conductivity, W/(m × K)

ρ = density, kg/m<sup>3</sup>

λ'<sub>μ</sub> = moisture conductivity by water chemical potential difference, kg/(m × s × J/kg)

λ'<sub>T</sub> = moisture conductivity by temperature difference, kg/(m × s × K)

ψ = moisture content, m<sup>3</sup>/m<sup>3</sup>

μ = water chemical potential (free water standard), J/kg

Subscript w = water; s = solid; g = gas; l = liquid; i = ice

Vapor and saturated water permeability are converted to permeability by water chemical potential (λ'<sub>μ,sat</sub>) in order to be used in the basic equations. When the tile is unsaturated, water permeability (λ'<sub>μ</sub>) is obtained by Equation (4). Higher linear factor A means that the water that penetrated into the tile body spreads faster.

The exponential factor N is set at 500 from the results of the previous investigation (Iba 2010).

$$\lambda'_{\mu} = A \times \psi_l + (\lambda'_{\mu,sat} - A \times \psi_{l,sat}) \times (\psi_l / \psi_{l,sat})^N \quad (4)$$

where

λ'<sub>μ</sub> = Unsaturated water permeability, kg/m s (J/kg)

λ'<sub>μ,sat</sub> = Saturated water permeability, kg/m s (J/kg)

ψ<sub>l</sub> = Liquid water content, m<sup>3</sup>/m<sup>3</sup>

ψ<sub>l,sat</sub> = Maximum moisture content, m<sup>3</sup>/m<sup>3</sup>

A = Linear factor

N = Exponential factor

### 3.2 Calculation Model and Material Properties

Figure 7 shows the section of a typical roof installed with roof tiles and the calculation model. An eave end tile is placed on the roof end, and other tiles are hung on the tile battens partially overlapping the lowermost tile. Generally, the undersurface of a roof tile is exposed to an air layer. Thus, both surfaces of the tile are assumed to be exposed to outdoor air in this calculation.

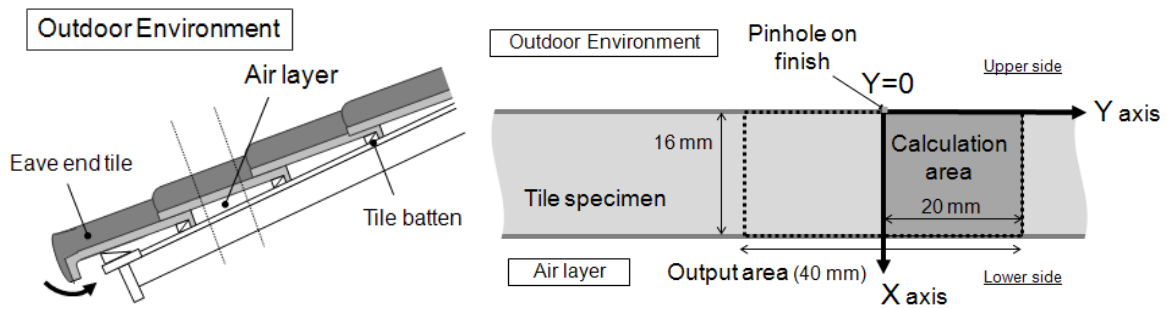


FIGURE 7: Section of a typical roof with roof tiles and the calculation model

A part of a tile with a surface finish on both sides is analyzed. The upper side contains a pinhole whose width is set at 0.1 mm (1/400 of the output area). The water resistance of the pinhole area is assumed to be extremely small than that of the surface finish. The calculation area and the output area are shown in Figure 7. The heat and moisture transfer properties of the tile body and surface finish are shown in Table 1.

TABLE 1: Heat and moisture transfer properties of the tile body and surface finish

Tile body	Thermal conductivity (dry condition)	0.937	W/m K
	Vapor permeability	$4.139 \times 10^{-12}$	kg/m s Pa
	Water permeability (saturated condition)	3.66	m/s
	Specific heat	920	J/kg K
	Density	2100	kg/m <sup>3</sup>
	Porosity (= Maximum moisture content)	26.2	%
Surface finish	Thermal resistance	Not considered	
	Vapor resistance	$5.35 \times 10^9$	m <sup>2</sup> s Pa/kg
	Water resistance	$9.92 \times 10^9$	m <sup>2</sup> s Pa/kg
Pinhole or	Vapor resistance (pinhole or unfinished surface)	$2.42 \times 10^6$	m <sup>2</sup> s Pa/kg
Unfinished surface	Water resistance (pinhole)	37015.0	m <sup>2</sup> s Pa/kg
	Water resistance (unfinished surface)	2677.8	m <sup>2</sup> s Pa/kg

Figure 8 shows the absorption isotherm of the tile body. The moisture condition is expressed by the water chemical potential instead of the relative humidity. The freezing temperature calculated by Equation (3) is also plotted. It can be observed that when the tile is nearly saturated (approximately 95% saturation), it can freeze at a temperature slightly below 0°C.

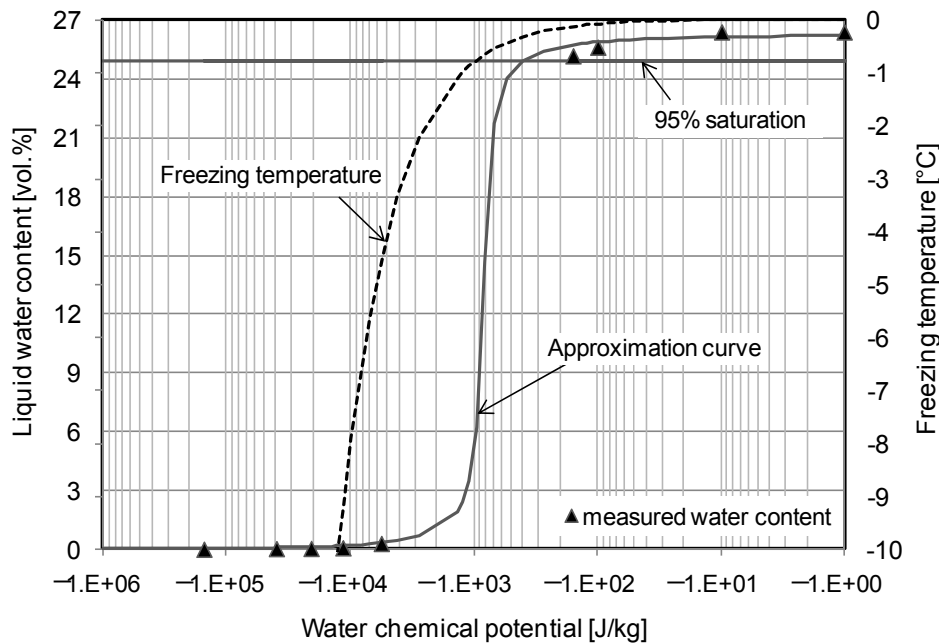


FIGURE 8: Absorption isotherm and freezing temperature

### 3.3 Calculation Conditions

The heat transfer coefficients are shown in Table 2. Because the air velocity in the air layer is considered to be lower than that of outdoor air, the convective heat transfer coefficient of the undersurface is set at a lower value than that of the upper surface. Moisture transfer coefficients on both surfaces are calculated using the Lewis relation.

When there is precipitation, the upper side of the tile is covered with a thin water film; thus, the boundary is assumed to be saturated where the water chemical potential is set at  $-0.1$  J/kg (nearly 0 J/kg).

TABLE 2: Boundary conditions

Upper surface	Convective heat transfer coefficient	18.60	W/m <sup>2</sup> K
	Radiative heat transfer coefficient	4.65*	W/m <sup>2</sup> K
Lower surface	Convective heat transfer coefficient	2.30	W/m <sup>2</sup> K
	Radiative heat transfer coefficient	4.65*	W/m <sup>2</sup> K

\*Design value of indoor heat transfer, assuming emissivity of material to be 0.9

The environmental conditions were determined considering the colder conditions of a warm area in Japan, in which the minimum outdoor air temperature is below 0 °C. In this calculation, a situation is modeled in which the outdoor temperature decreases linearly to  $-2.0$  °C after a small amount of precipitation. Solar radiation is not considered since the weather is assumed rainy or cloudy through the periods. In order to simplify the analysis, night-sky radiation is not also considered, because the amount of radiation depends on the slope and the emissivity of the roof. The determined temperature, humidity, and precipitation are shown in Figure 9.

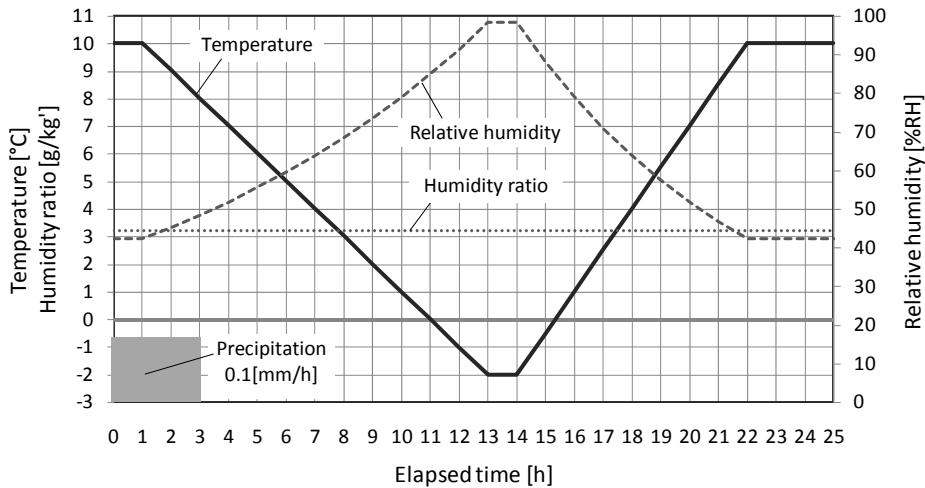


FIGURE 9: Environmental conditions

To examine the influence of the surface finish and moisture permeability, four patterns of calculation were conducted as shown in Table 3. Moisture diffusion in the tile body becomes faster as a parameter A, which is a linear factor in Equation (4), increases. When the undersurface is unfinished, the moisture in the tile can easily evaporate through it.

TABLE 3: Calculation patterns

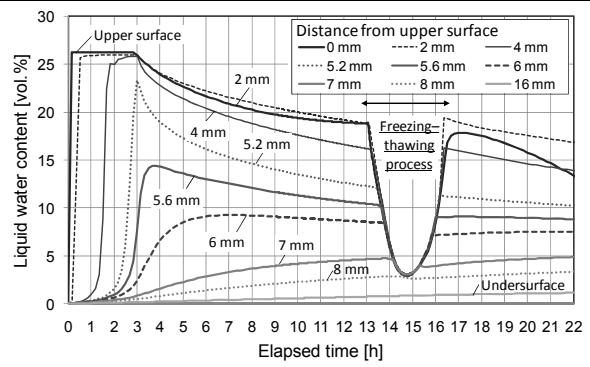
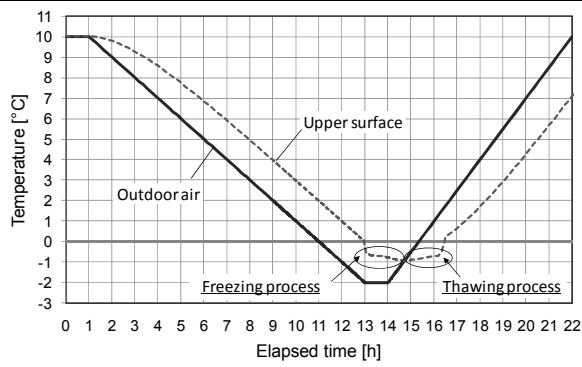
Pattern No.	Surface finish	Parameter A	Note
a-1	Both surfaces	$5.0 \times 10^{-10}$	
a-2	Both surfaces	$2.5 \times 10^{-9}$	A: $\times 5$ of a-1
b-1	Only upper surface	$5.0 \times 10^{-10}$	
b-2	Only upper surface	$2.5 \times 10^{-9}$	A: $\times 5$ of b-1

### 3.4. Results

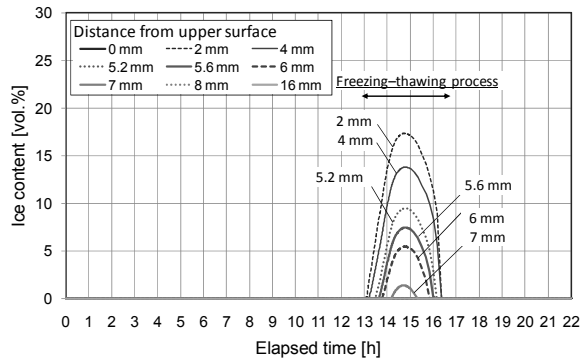
The time profiles of temperature, liquid water, ice and total moisture contents in Pattern a-1 are shown in Figure 10. Total moisture content is the sum of the liquid water and ice contents. These are the results for the position  $Y = 0$  (along X-axis). Because the tile thickness is relatively low (16 mm), the temperature of the inside and undersurface of the tile is almost the same as that of the upper surface. In both the freezing and thawing processes, the temperature changes gradually compared with those without phase changes.

The liquid water content increases from the upper surface to the inside in about 3 h because of rain penetration. When the temperature reaches the freezing point, freezing occurs in the high water content zone. In Pattern a-1, freezing occurs up to a depth of 7 mm in the upper surface.

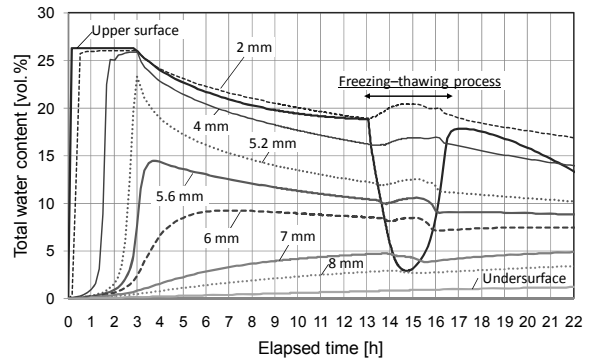
Although volume expansion of water due to freezing is not considered in this calculation, the total moisture content slightly increases in the freezing zone. This is because the liquid water content decreases during the freezing process, which causes a decrease in the water chemical potential, and unfrozen water flows into the freezing zone from a neighboring unfrozen zone. In the zone closest to the pinhole ("Upper surface" in Figure 10), freezing does not occur because of decrease in water content due to an outflow to the freezing area and evaporation.



Temperature



Liquid water content



Ice content

Total moisture content

FIGURE 10: Time profile for Pattern a-1

Figures 11 and 12 show the change in liquid water content distribution 1, 3, 8, and 13 h after the start of Pattern a-1 and Pattern a-2 calculations, respectively. The high water content zone spreads to approximately 3 mm depth and 8 mm width around the pinhole after 1 h of rain. When 3 h elapse, the area expands up to 6 mm depth and 12 mm width. During the rain, the area with high water content can be clearly distinguished.

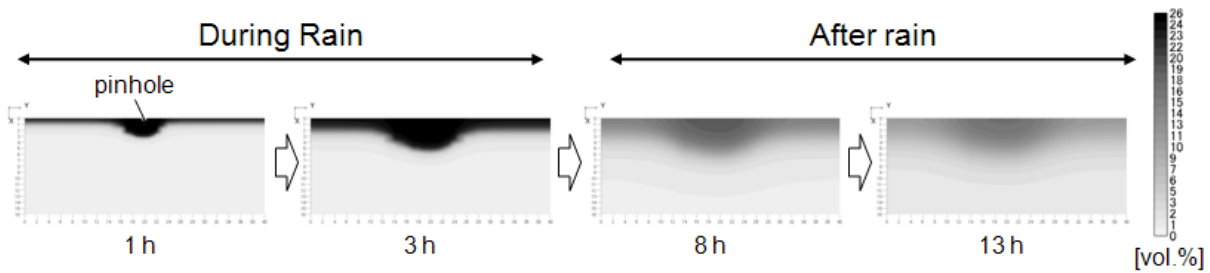


FIGURE 11: Change in moisture distribution in Pattern a-1 (before freezing)

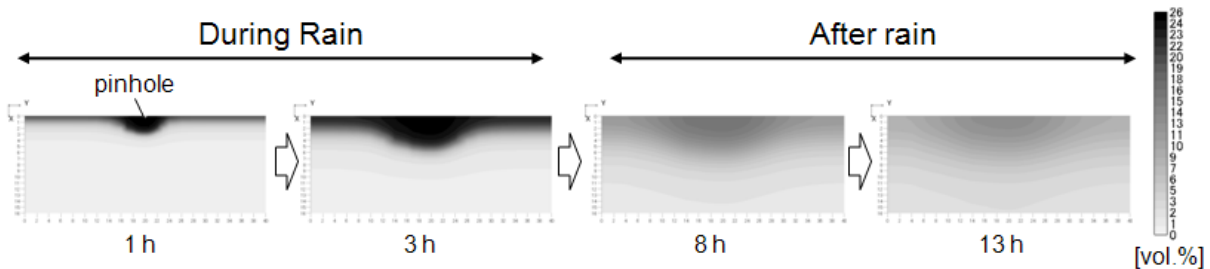


FIGURE 12: Change in moisture distribution in Pattern a-2 (before freezing)

After the rain stops, liquid water around the pinhole moves inside the tile body, which remains dry, and evaporates through the surface finish, especially, the pinhole. Because moisture diffuses faster in Pattern a-2, the high water content area becomes indistinguishable.

Figure 13 shows the liquid water content distribution before freezing at the position  $Y = 0$  (along X-axis) in all calculation patterns. When the moisture permeability is smaller (Patterns a-1 and b-1), the difference in distributions is not influenced by the surface finish position. When moisture moves faster (Patterns a-2 and b-2), water penetrates to a larger distance from the upper surface through the pinhole. Because the undersurface is unfinished in Pattern b-2, moisture inside the tile can easily evaporate from the undersurface; therefore, the water content near the undersurface is lower than that in Pattern a-2.

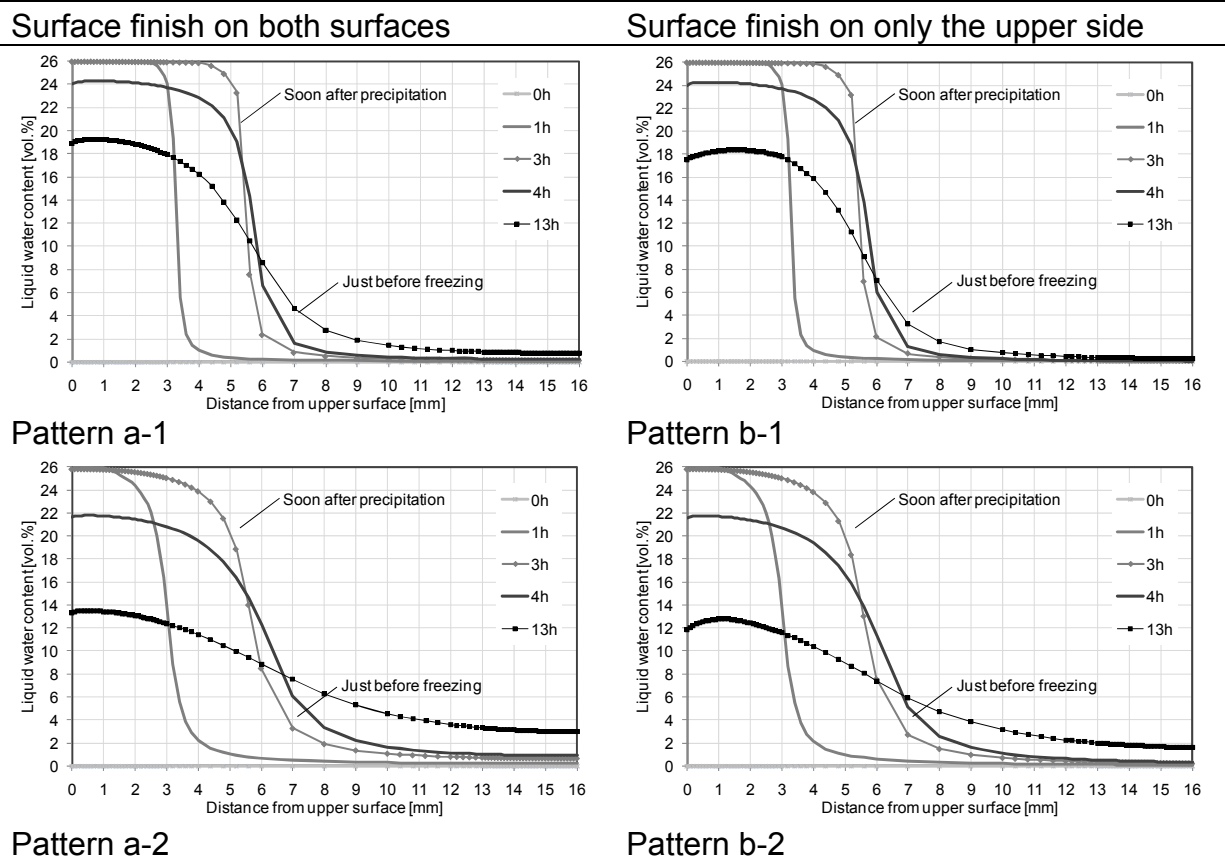
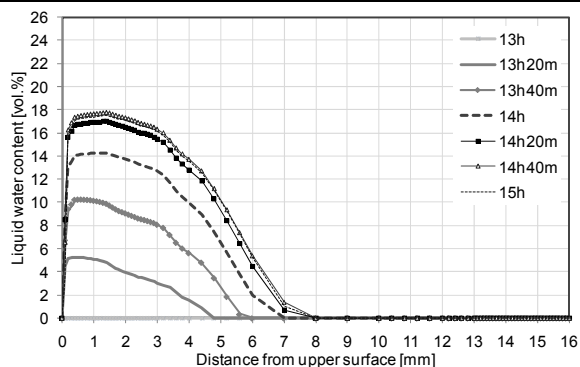


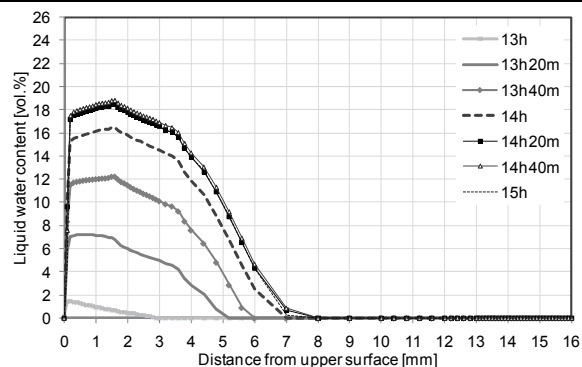
FIGURE 13: Liquid water content distribution before freezing ( $Y = 0$ )

Figure 14 shows the ice content distribution during the freezing process. When the temperature and the water chemical potential (corresponding to the liquid water content) satisfy the freezing condition defined by Equation (3), ice formation starts at the zone. Latent heat is generated in the freezing zone; thus, the temperature increases slightly. Furthermore, as described before, because unfrozen water flows into the freezing zone from a neighboring unfrozen zone and the water content increases, ice grows with time. The amount of ice formation is determined according to the heat and moisture transfer balance.

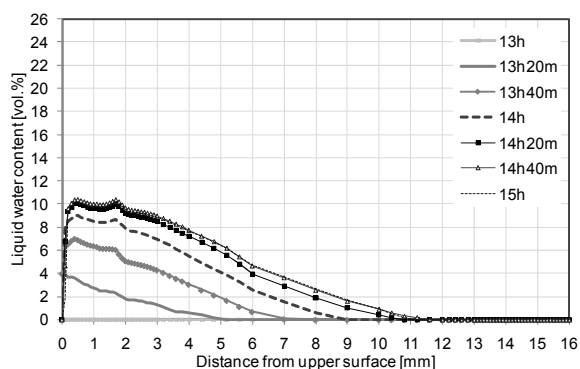
Surface finish on both surfaces



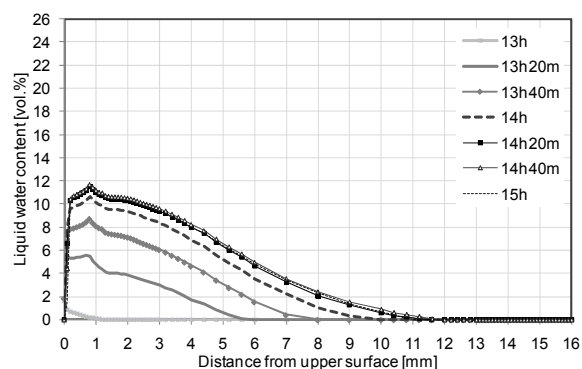
Surface finish on only the upper side



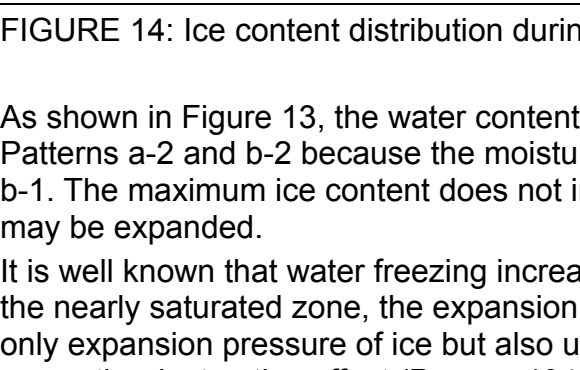
Pattern a-1



Pattern b-1



Pattern a-2



Pattern b-2

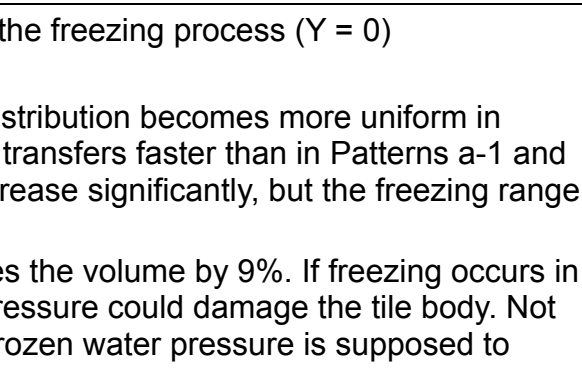


FIGURE 14: Ice content distribution during the freezing process ( $Y = 0$ )

As shown in Figure 13, the water content distribution becomes more uniform in Patterns a-2 and b-2 because the moisture transfers faster than in Patterns a-1 and b-1. The maximum ice content does not increase significantly, but the freezing range may be expanded.

It is well known that water freezing increases the volume by 9%. If freezing occurs in the nearly saturated zone, the expansion pressure could damage the tile body. Not only expansion pressure of ice but also unfrozen water pressure is supposed to cause the destructive effect (Powers 1945).

As even a small pinhole can allow significant amounts of water to penetrate into the tile body, the moisture content will show non-uniform distribution if such pinholes are randomly distributed on the surface finish. This could be one reason for small spallings or flaking in an actual situation.

#### 4. CONCLUSIONS

In this study, the characteristics and causes of frost damage in roof tiles were investigated through water penetration experiments, a freezing–thawing test, and a numerical analysis.

In the water penetration experiment, the distributions of water in the tile were experimentally examined. The results showed that the water content might increase in particular small areas. The results of the new freezing–thawing test with different water supplies revealed that even small water droplets could penetrate the finish and could cause spalling similar to that found in the field.

Furthermore, the time profile and the distributions of liquid water and ice content in the freezing–thawing process were analyzed. The analysis was based on equations of simultaneous heat and moisture transfers which consider freezing and thawing. The influence of the surface finish position (on both surfaces or on only the upper side) and water permeability in the tile body were also considered.

The results showed that when the water permeability is small, high local water content tended to occur. It is considered that high water content increases the risk of frost damage. This information about hygrothermal properties of the surface finish and the tile body will help in material development and advancement in the future.

## ACKNOWLEDGMENTS

This research was partially supported by the Ministry of Education, Culture, Sports, Science, and Technology, Grant-in-Aid for Scientific Research (A), 18206062, 2006 and Scientific Research (B), 18404013, 2006.

## REFERENCES

- Iba, C., 2010. A basic study on characteristics of moisture transfer and freezing –thawing process in roof tiles in warm areas (in Japanese), Doctoral dissertation, Kyoto University, pp. 121-126.
- Iba, C. and Hokoi, S. 2003. Freezing-thawing processes in a brick wall in relatively warm area of Japan. Proceedings of the 2nd International Conference on Building Physics, Leuven, pp. 257-266.
- Iba C. and Hokoi S. 2006. Frost damage of roof tiles in relatively warm area in Japan – Condensation on external surface. Proceedings of 12th Symposium for Building Physics, Vol.1, pp.120-127.
- Iba C. and Hokoi S. 2009. Measurement of water permeability of roof tiles and influence of entrapped air. Journal of ASTM International, Vol.6, No.9, paper ID: 001909JAI.
- Iba C. and Hokoi S. 2011, Frost damage in roof tiles in relatively warm areas in Japan: water absorption and freezing-thawing experiments. Proceedings of the 9th Nordic Symposium on Building Physics, Vol.1, NSB 2011, pp. 231-238.
- Matsumoto M., Gao Y. and Hokoi S. 1993. Simultaneous heat and moisture transfer during freezing-melting in building materials, CIB/W40 meeting, Budapest, Sept. 1993
- Powers T.C. 1945. A working hypothesis for further studies of frost resistance of concrete, Journal of the American Concrete Institute, Vol. 16, No. 4: pp. 245-272.